BNL-NT-03/20
RBRC-333
September 2003

Longitudinally Polarized Photoproduction of Inclusive Hadrons Beyond the Leading Order

B. Jäger[a], M. Stratmann[a], and W. Vogelsang[b,c]

[a] *Institut für Theoretische Physik, Universität Regensburg, D-93040 Regensburg, Germany*

[b] *Physics Department, Brookhaven National Laboratory, Upton, New York 11973, U.S.A.*

[c] *RIKEN-BNL Research Center, Bldg. 510a, Brookhaven National Laboratory, Upton, New York 11973 – 5000, U.S.A.*

Abstract

We present a complete next-to-leading order QCD calculation for single-inclusive large-p_T hadron production in longitudinally polarized lepton-nucleon collisions, consistently including "direct" and "resolved" photon contributions. This process could be studied experimentally at a future polarized lepton-proton collider like eRHIC at BNL. We examine the sensitivity of such measurements to the so far completely unknown parton content of circularly polarized photons.

I Introduction

The successful start of the RHIC spin program marks a new era in spin physics. Very inelastic pp collisions at high energies open up unequaled possibilities to thoroughly address many interesting questions, most importantly perhaps those concerning the still unknown role of polarized gluons [1]. QCD analyses of upcoming high-p_T prompt photon, jet, heavy flavor, inclusive-hadron, and $W^{\pm}$ boson production data will greatly deepen and enrich the understanding of the nucleon and of QCD that we had gained previously from polarized deeply-inelastic scattering (DIS) of leptons off nucleons.

Investigations of interactions between polarized leptons and nucleons will, however, continue to play a vital role in spin physics. Besides the many observables of DIS, *photoproduction* processes are particularly interesting. They give access to the parton content of circularly polarized photons, due to the presence of contributions to the cross section where the photon "resolves" into its parton content, for instance, by fluctuating into a vector meson of the same quantum numbers, prior to the hard QCD interaction. Such contributions compete with the "direct" part, for which the photon simply interacts as an elementary pointlike particle.

It is well-known [2] that at lower (fixed-target) energies, the direct component tends to dominate over the resolved one. Only at collider energies do resolved contributions become important. Extensive studies in the unpolarized case at the HERA and LEP colliders have firmly established the concept of photonic parton densities [3] and shown that resolved photon processes contribute a sizable fraction of photoproduction events in certain kinematic regions. The fact that e^+e^- and ep data can be universally described by the same set of photonic parton densities marks an important test and success of QCD.

It has not yet been possible to observe resolved contributions for *polarized* photons, due to the fact that only fixed-target lepton-nucleon experiments have been performed so far in the polarized case. In this context, an exciting possibility would be to have a polarized lepton-proton *collider* such as the planned eRHIC project at BNL [4], which is currently under discussion.

Motivated by this prospect, we present in this paper a study for photoproduction of single-inclusive high-p_T hadrons at a future lepton-proton collider with longitudinally polarized beams, and investigate the sensitivity of this reaction to the contribution from resolved photons. We had made first exploratory studies of this, and related, reactions in [5]. Our present study goes beyond the results of [5] in that we now consistently include both the direct and the resolved photon processes in the next-to-leading order (NLO) of QCD. This is crucial for reliable quantitative analyses in the future as theoretical uncertainties are expected to be under much better

control beyond the lowest order (LO) approximation of QCD. For the resolved contribution, the NLO corrections to polarized QCD hard-scattering have become available only recently in [6, 7]. For the polarized direct component, the corresponding cross sections were already calculated some time ago in [8]. We have rederived the expressions and agree with the published results. In addition to extending our study to NLO, we also tailor our phenomenological results to the eRHIC situation.

In the next section we sketch the technical framework for the description of polarized photoproduction reactions. Section III is devoted to numerical studies for the eRHIC. We conclude in Section IV.

II Technical Framework

We consider the spin-dependent photoproduction cross section for the reaction $lp \to l'HX$, where the hadron H is at high transverse momentum p_T, ensuring a large momentum transfer. We may then write the differential cross section in a factorized form:

$$\begin{aligned}
\frac{d\Delta\sigma}{dp_T d\eta} &= \frac{1}{2}\left[\frac{d\sigma_{++}}{dp_T d\eta} - \frac{d\sigma_{+-}}{dp_T d\eta}\right] \\
&= \frac{2p_T}{S}\sum_{a,b,c}\int_{1-V+VW}^{1}\frac{dz}{z^2}\int_{VW/z}^{1-(1-V)/z}\frac{dv}{v(1-v)}\int_{VW/vz}^{1}\frac{dw}{w}\Delta f_a^l(x_l,\mu_f)\Delta f_b^p(x_p,\mu_f)D_c^H(z,\mu_f') \\
&\times \left[\frac{d\Delta\hat{\sigma}_{ab\to cX}^{(0)}(s,v)}{dv}\delta(1-w) + \frac{\alpha_s(\mu_r)}{\pi}\frac{d\Delta\hat{\sigma}_{ab\to cX}^{(1)}(s,v,w,\mu_r,\mu_f,\mu_f')}{dvdw}\right] . \qquad (1)
\end{aligned}$$

This generic form applies to both the direct and the resolved cases. The subscripts "++" and "+−" denote the helicities of the colliding lepton and proton, μ_r the renormalization scale, and $S \equiv (P_l + P_p)^2$ the available c.m.s. energy squared. Neglecting all masses, V and W in Eq. (1) can be expressed in terms of the c.m.s. pseudorapidity η and transverse momentum p_T of the observed hadron:

$$V = 1 - \frac{p_T}{\sqrt{S}}e^{\eta} \quad \text{and} \quad W = \frac{p_T^2}{SV(1-V)} \quad . \qquad (2)$$

We count positive rapidity in the proton's forward direction.

The sum in Eq. (1) is over all partonic channels $a + b \to c + X$ contributing to the single-inclusive cross sections, with $d\Delta\hat{\sigma}_{ab\to cX}^{(0)}$ and $d\Delta\hat{\sigma}_{ab\to cX}^{(1)}$ the associated polarized LO and NLO partonic cross sections, respectively. For the direct contribution to the cross section, depicted in Fig. 1 (a), we have $a = \gamma$, while for the resolved ones [see Fig. 1 (b)] a stands for the parton

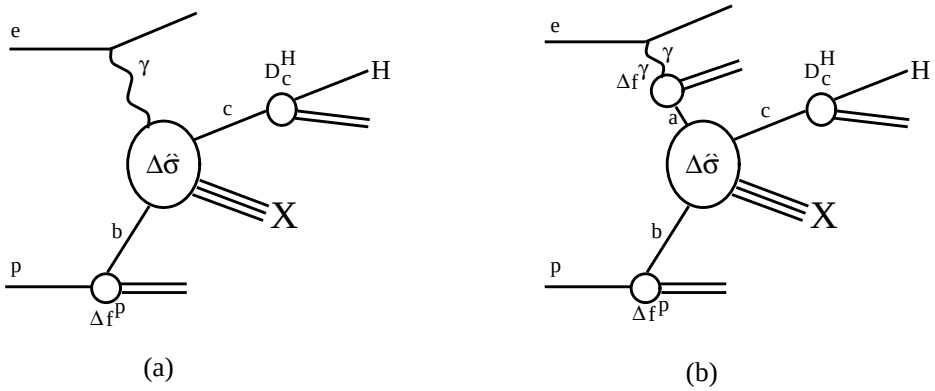

Figure 1: Generic direct (a) and resolved (b) photon contributions to the process $lp \to l'HX$.

emerging from the photon. For convenience, we introduce effective polarized parton densities, $\Delta f_a^l(x_l, \mu_f)$, in the lepton, with x_l the fraction of the lepton momentum carried by parton a and μ_f the factorization scale. The $\Delta f_a^l(y, \mu_f)$ are defined via the convolution

$$\Delta f_a^l(x_l, \mu_f) = \int_{x_l}^1 \frac{dy}{y} \Delta P_{\gamma l}(y) \Delta f_a^\gamma \left(x_\gamma = \frac{x_l}{y}, \mu_f \right) \quad , \tag{3}$$

with

$$\Delta P_{\gamma l}(y) = \frac{\alpha_{em}}{2\pi} \left\{ \left[\frac{1-(1-y)^2}{y} \right] \ln \frac{Q^2_{\max}(1-y)}{m_l^2 y^2} + 2m_l^2 y^2 \left(\frac{1}{Q^2_{\max}} - \frac{1-y}{m_l^2 y^2} \right) \right\} \tag{4}$$

being the spin-dependent Weizsäcker-Williams "equivalent photon" spectrum including its non-logarithmic contributions[1] [9]. Here, m_l is the lepton mass and $Q_{\max}$ the allowed upper limit on the radiated photon's virtuality, to be fixed by the experimental conditions. For the direct case, one simply replaces

$$\Delta f_a^\gamma(x_\gamma, \mu_f) \;\to\; \delta(1 - x_\gamma) \; , \tag{5}$$

while in the resolved contribution the yet unmeasured parton distributions of circularly polarized photons occur that are the focus of this paper. Likewise, $\Delta f_b^p(x_p, \mu_f)$ denotes the density of parton b in the polarized proton, and $D_c^H(z, \mu'_f)$ is the usual unpolarized fragmentation function for parton c going into the observed hadron H, at scale μ'_f. The relations between parton-level and hadron-level variables are

$$s \equiv (p_a + p_b)^2 = x_l x_p S \;\; , \;\; x_l = \frac{VW}{vwz} \;\; , \quad x_p = \frac{1-V}{z(1-v)} \;\; . \tag{6}$$

As we mentioned earlier, it is a main feature of our paper that for the first time we include both the direct and the resolved contributions to the polarized cross section at NLO, as indicated

[1]The latter turn out to be numerically unimportant in our study, but we keep them for completeness.

by the first-order corrections $d\Delta\hat{\sigma}^{(1)}_{ab\to cX}$ in Eq. (1). The actual calculation of these corrections is generally a formidable task. Since later on we will mainly consider spin asymmetries, we also need the corresponding spin-averaged partonic cross sections. Let us go through the various ingredients that we need in a little more detail.

The resolved contribution is technically equivalent to a hadroproduction cross section such as $pp \to HX$. The corresponding $d\Delta\hat{\sigma}^{(1)}_{ab\to cX}$ may therefore be immediately adopted from our recent calculation [6] for this case. In that reference, we also re-derived the (previously known [10]) expressions for the unpolarized case. There are in total 16 different partonic channels.

The NLO contributions to the direct-photon component have been calculated in [11, 12] and [8] for the unpolarized and polarized cases, respectively. Having the techniques available that we used in [6], it was a straightforward, though tedious, work to check the old results from the scratch. For the polarized case we fully agree with [8], at an analytical level. In the unpolarized case, we were able to identify some minor mistakes (beyond those noted in [8]) in the computer code of [12]; apart from those we agree with that calculation as well.

The technical details of the NLO calculation for the direct part may be found in [8]. We will not repeat these here, but will only recall an important aspect of photoproduction cross sections beyond the LO: writing the cross section as the sum of the direct and the resolved photon contributions,

$$d\Delta\sigma = d\Delta\sigma_{\rm dir} + d\Delta\sigma_{\rm res} \quad , \tag{7}$$

we emphasize that neither $d\Delta\sigma_{\rm dir}$ nor $d\Delta\sigma_{\rm res}$ are *individually* physical, i.e., experimentally measurable. This can be easily seen by noticing that the $2 \to 3$ contributions to the direct cross section have singular configurations arising from a collinear splitting of the incoming photon into a quark-antiquark pair. These contributions are absorbed, according to the factorization theorem, into the so-called "pointlike" part of the NLO photonic parton densities and thus into the *resolved* component. The subtraction of the singular part is unique only up to finite pieces, and the ensuing ambiguity (i.e., the choice of "factorization scheme") cancels only when the direct and resolved parts are combined.

As an example, when using dimensional regularization ($d = 4-2\varepsilon$), the appropriate "counter cross section" that cancels the $\gamma \to q\bar{q}$ collinear singularity in the subprocess $\gamma\bar{q} \to gX$ is schematically given by

$$\frac{d\Delta\hat{\sigma}^{\rm counter}_{\gamma\bar{q}\to gX}}{dvdw} \sim -\frac{\alpha_{em}}{2\pi}\,\Delta H_{q\gamma} \otimes d\Delta\hat{\sigma}_{q\bar{q}\to gg} \tag{8}$$

where $d\Delta\hat{\sigma}_{q\bar{q}\to gg}$ is the polarized Born cross section for the reaction $q\bar{q} \to gg$ in d dimensions,

and (e_q denotes the quark charge)

$$\Delta H_{q\gamma}(x,\mu_f) = \left(-\frac{1}{\varepsilon} + \gamma_E - \ln 4\pi\right) 3e_q^2\,[2x-1]\left(\frac{s}{\mu_f^2}\right)^{\varepsilon} + \Delta h_{q\gamma}(x) \quad . \tag{9}$$

The freedom in the choice of the factorization prescription is reflected by the arbitrary finite piece $\Delta h_{q\gamma}(x)$ which may be subtracted alongside the singular $1/\varepsilon$ contribution. For the $\overline{\rm MS}$ convention, $\Delta h_{q\gamma}(x) = 0$. An alternative factorization scheme (DIS$_\gamma$) was proposed in the unpolarized case [13] to facilitate the analysis of data on the DIS photon structure function F_2^γ. Here the photonic Wilson coefficient $C_{2,\gamma}$ in the NLO expression for F_2^γ is absorbed into the definition of the quark distributions of the photon. A similar scheme can be set up in the polarized case as well [14] by subtracting the corresponding polarized coefficient function $\Delta C_{1,\gamma}$ in the structure function g_1^γ. The photonic parton densities in the $\overline{\rm MS}$ and DIS$_\gamma$ schemes are then related in the following way [14]:

$$\Delta f_a^{\gamma,\overline{\rm MS}}(x,\mu_f) = \Delta f_a^{\gamma,{\rm DIS}_\gamma}(x,\mu_f) + \delta\Delta f_a^\gamma(x) \quad , \tag{10}$$

where

$$\begin{aligned} \delta\Delta f_q^\gamma(x) &= \delta\Delta f_{\bar q}^\gamma(x) = -2N_C e_q^2 \frac{\alpha_{em}}{4\pi}\left[(2x-1)\left(\ln\frac{1-x}{x} - 1\right) + 2(1-x)\right] \quad , \\ \delta\Delta f_g^\gamma(x) &= 0 \quad . \end{aligned} \tag{11}$$

The relation between the partonic cross sections for the direct contribution reads accordingly:

$$d\Delta\hat\sigma_{\gamma b\to cX}^{{\rm DIS}_\gamma} = d\Delta\hat\sigma_{\gamma b\to cX}^{\overline{\rm MS}} + \sum_a \delta\Delta f_a^\gamma \otimes d\Delta\hat\sigma_{ab\to cX} \tag{12}$$

with $\delta\Delta f_a^\gamma$ given above and the symbol $\otimes$ denoting a standard convolution. The $d\Delta\hat\sigma_{ab\to cX}$ are the appropriate LO partonic cross sections. For the resolved cross section all partonic cross sections remain unaffected by this transformation. It is straightforward to verify that the scheme transformation indeed leaves the physical cross section in Eq. (7) invariant.

Our explicit analytical expressions for the polarized NLO subprocess cross sections for the direct and resolved cases are too lengthy to be given here, but can be found in our computer code which is available upon request.

III Numerical Results

Let us now turn to a first numerical application of our analytical results. Instead of presenting a full-fledged phenomenological study of single-inclusive hadron production in polarized lp collisions, we only focus on the most interesting questions: the importance of the NLO corrections,

the dependence on unphysical scales, and the sensitivity to the yet unmeasured parton densities of circularly polarized photons.

For all our calculations we choose a c.m.s. energy of $\sqrt{S} = 100\,\mathrm{GeV}$ as planned for polarized electron-proton collisions at eRHIC. We limit ourselves to the case of neutral pions (π^0); extension to other hadrons would be straightforward. We will always perform the NLO (LO) calculations using NLO (LO) parton distribution functions, fragmentation functions, and the two-loop (one-loop) expression for α_s. The value for α_s is taken according to our choice of proton parton distributions, which is CTEQ5 [15] for the unpolarized case and GRSV [16] for the polarized one.

In the equivalent photon spectrum in Eq. (4) we use similar parameters as the H1 and ZEUS experiments at HERA. We employ $Q^2_{\mathrm{max}} = 1\,\mathrm{GeV}^2$ and take the photon momentum fraction to be within $0.2 \leq y \leq 0.85$.

The fragmentation functions for neutral pions, D_c^π, have been determined with some accuracy from analyses of data for pion production in e^+e^- collisions [17, 18]. Even though our knowledge of the D_c^π certainly still needs improvement, we assume for this study that the fragmentation functions will be well known by the time experiments at a future polarized lepton-proton collider are carried out. For our analysis we take the LO and NLO sets of Ref. [17] which also yield good agreement with recent high-p_T data for $pp \to \pi^0 X$ at $\sqrt{S} = 200\,\mathrm{GeV}$ by the PHENIX collaboration [19].

Since the parton distributions Δf^γ of circularly polarized photons are completely unmeasured so far, we have to invoke some model for them. Two extreme scenarios were considered in [20, 5], with "maximal" [$\Delta f^\gamma(x,\mu_0) = f^\gamma(x,\mu_0)$] and "minimal" [$\Delta f^\gamma(x,\mu_0) = 0$] saturation of the "positivity constraint" $|\Delta f^\gamma(x,\mu_0)| \leq f^\gamma(x,\mu_0)$. μ_0 denotes the scale where the boundary conditions [20] for the evolution are specified. For the spin-averaged densities f^γ the phenomenologically successful GRV photon distributions [21] were used. We employ these two extreme sets for the Δf^γ in Eq. (3), along with appropriate LO [20] and NLO [14, 22] boundary conditions and evolution equations. Our default choice for the numerical studies will be the "maximal" set.

As we already pointed out in previous LO studies [5], for single-inclusive measurements rapidity differential cross sections are particularly suited for extracting the resolved contributions and hence the polarized photonic parton distributions. This can be easily understood by looking at the momentum fractions of the photon and proton distributions as a function of rapidity. As we count positive rapidity in the proton's forward direction, large $x_\gamma \to 1$ are

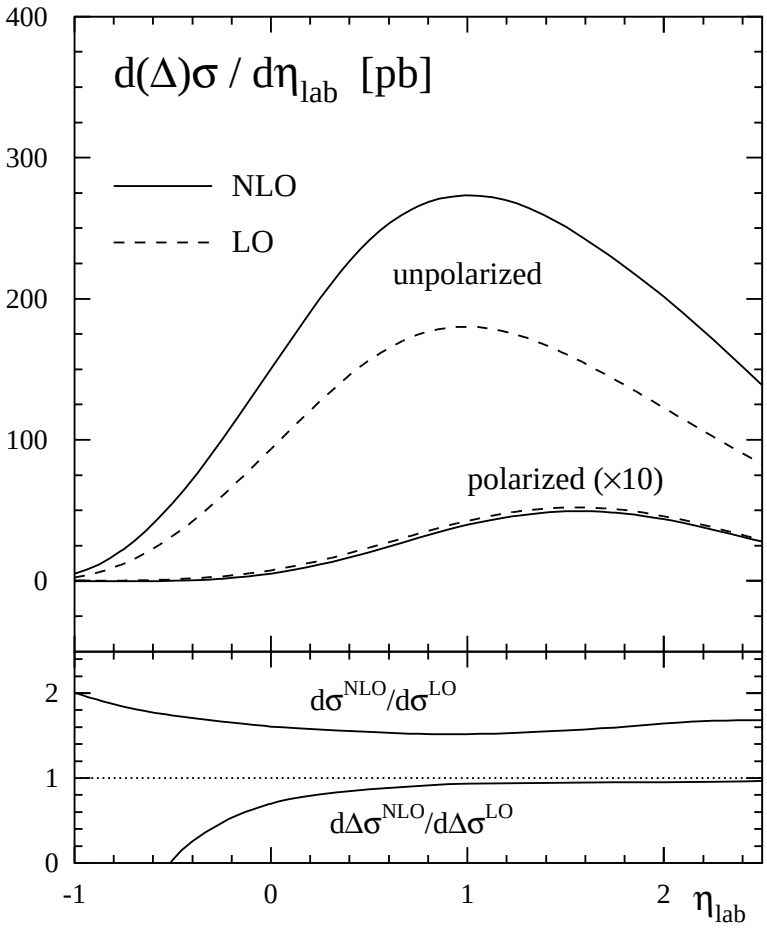

Figure 2: Unpolarized and polarized π^0 photoproduction cross sections in NLO (solid lines) and LO (dashed lines) at $\sqrt{S} = 100$ GeV. The polarized results are enlarged by a factor of 10. The lower panel shows the ratios of the NLO and LO results in each case.

probed at large negative rapidities. Here one expects no difference between the two photon scenarios since the cross section is dominated by the direct photon contribution sitting strictly at $x_\gamma = 1$. In addition, in the region $x_\gamma \to 1$ the Δf^γ are dominated by the "pointlike" part which only depends on the starting scale μ_0 but not on the details of the hadronic input. On the other hand, for large and positive rapidities small x_γ values are probed, and the resolved contribution is expected to dominate more and more.

Figure 2 shows our results for the unpolarized and polarized photoproduction cross sections for neutral pions at LO and NLO at $\sqrt{S} = 100\,\mathrm{GeV}$ as functions of the laboratory-frame pseudorapidity η_{lab}. For the asymmetric eRHIC kinematics ($E_p = 250\,\mathrm{GeV}$, $E_e = 10\,\mathrm{GeV}$), η_{lab} is related to the c.m.s. frame rapidity via

$$\eta_{\mathrm{lab}} = \eta + \frac{1}{2} \ln \frac{E_p}{E_e} \quad . \tag{13}$$

We have integrated over the transverse momentum $p_T \geq 4\,\mathrm{GeV}$ of the produced pion. All scales

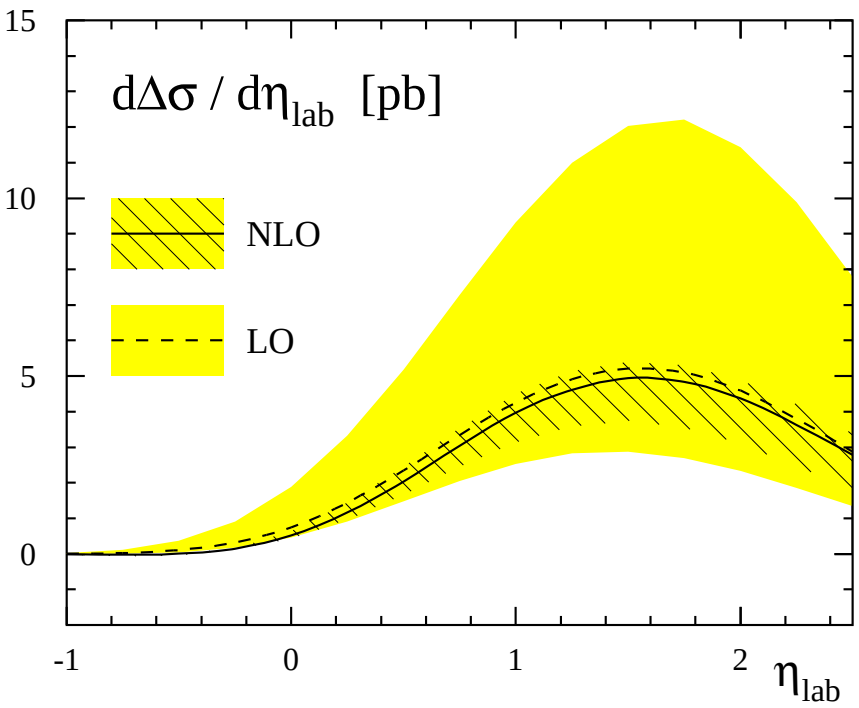

Figure 3: Scale dependence of the polarized cross section for π^0 production at LO and NLO in the range $p_T/2 \leq \mu_r = \mu_f = \mu'_f \leq 2p_T$. The solid and dashed lines correspond to the choice where all scales are set to p_T.

have been set equal: $\mu_r = \mu_f = \mu'_f = p_T$.

The lower part of the figure displays the so-called "K-factor"

$$K = \frac{d(\Delta)\sigma^{\rm NLO}}{d(\Delta)\sigma^{\rm LO}} \quad . \tag{14}$$

One can see that in the unpolarized case the corrections are roughly constant, of size $60\% - 80\%$ over most of the $\eta_{\rm lab}$ region considered. In the polarized case, we find generally much smaller corrections, at least for the above choice of scales. Only for negative $\eta_{\rm lab}$ where the cross section changes sign are the corrections large.

An important reason why inclusion of the NLO corrections is generally vital is that they are expected to considerably reduce the dependence of the cross sections on the unphysical factorization and renormalization scales. This improvement in scale dependence when going from LO to NLO is a measure of the impact of the NLO corrections, the residual scale dependence at NLO perhaps providing a rough estimate of the relevance of even higher order QCD corrections. Figure 3 shows the scale dependence of the spin-dependent cross section at LO and NLO. In each case the shaded bands indicate the uncertainties from varying the unphysical scales in the range $p_T/2 \leq \mu_r = \mu_f = \mu'_f \leq 2p_T$. The solid lines are for the choice where all

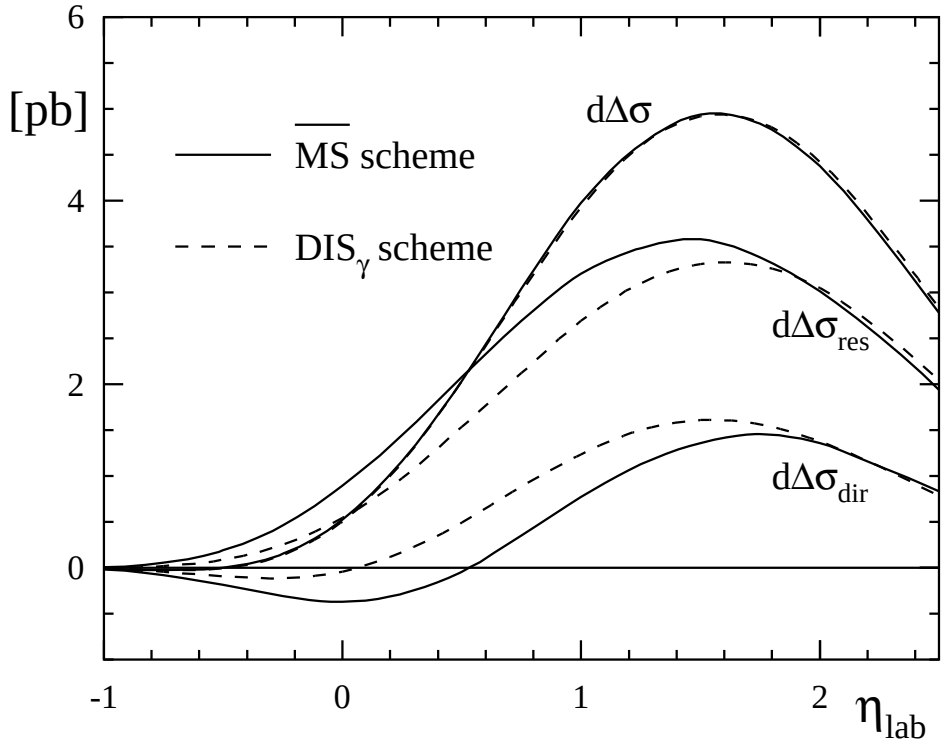

Figure 4: NLO direct and resolved photon contributions in the $\overline{\text{MS}}$ and DIS$_\gamma$ factorization schemes. Also shown is their sum which has to be independent of theoretical conventions.

scales are set to p_T. One can see that the scale dependence indeed becomes much smaller at NLO and that the lowest order approximation may capture the main features of the process but will not provide a satisfactory quantitative understanding.

Figure 4 demonstrates, as discussed in Section II, that the direct and resolved contributions individually depend on the choice of the factorization scheme, but that the physical, i.e., experimentally accessible, cross section does not. To make this point, we transform the polarized cross sections from the $\overline{\text{MS}}$ to the DIS$_\gamma$ scheme as described in Eqs. (10)-(12).

A first determination of the parton content of circularly polarized photons could be one of the key physics goals of the spin physics program at a future lepton-proton collider. Figure 5 shows the experimentally relevant spin asymmetry

$$A_{LL}^{\pi} = \frac{d\Delta\sigma}{d\sigma} = \frac{d\sigma_{++} - d\sigma_{+-}}{d\sigma_{++} + d\sigma_{+-}} \tag{15}$$

for π^0 photoproduction at eRHIC. As before we have integrated over $p_T \geq 4\,\text{GeV}$ and have chosen all scales to be p_T. At positive rapidities the spin asymmetry shows the expected dependence on the choice of the polarized photon densities. In order to be able to judge whether a future measurement can resolve such a difference we also give in Figure 5 an estimate for the

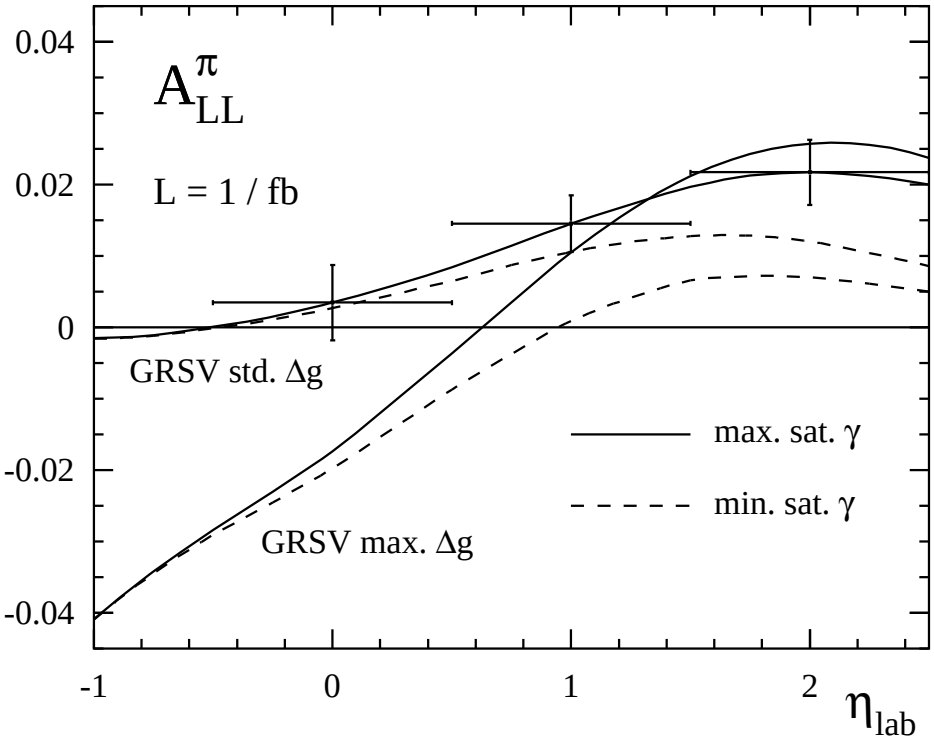

Figure 5: Spin asymmetry for π^0 photoproduction in NLO QCD for the two extreme sets of polarized photon densities and two different choices of spin-dependent proton distributions. The "error bars" indicate the statistical accuracy anticipated for eRHIC assuming an integrated luminosity of $1\,\mathrm{fb}^{-1}$.

expected statistical errors:

$$\delta A_{LL}^{\pi} \simeq \frac{1}{\mathcal{P}_e \mathcal{P}_p \sqrt{\mathcal{L}\sigma_{\mathrm{bin}}}}\,, \tag{16}$$

where $\mathcal{P}_e$ and $\mathcal{P}_p$ are the polarization of the lepton and proton beam, respectively, $\mathcal{L}$ denotes the integrated luminosity of the collisions, and σ_{bin} is the unpolarized cross section integrated over bins in η_{lab}. We have used $\mathcal{P}_{e,p} = 0.7$ and $\mathcal{L} = 1/\mathrm{fb}$, which are targets for eRHIC. It should be noted that an integrated luminosity of $\mathcal{L} = 1/\mathrm{fb}$ is expected to be accumulated after only a few weeks of running so that the statistical accuracy may eventually be much better than the one shown in Fig. 5.

To demonstrate that the sensitivity to Δf^{γ} is not masked by the dependence on the spin-dependent *proton* densities, we show in Fig. 5 also the results obtained for the GRSV "max. Δg" set [16], which is characterized by a much larger gluon density Δg than the one in the GRSV "standard" set. It is evident that at large positive rapidities the asymmetry is indeed mainly determined by the polarized photon structure. In the region of $\eta_{\mathrm{lab}} \leq 0$ a measurement of A_{LL}^{π} would be also an excellent source of information on the polarized gluon density in the nucleon. We note that, in any case, by the time eRHIC is commissioned we expect the spin

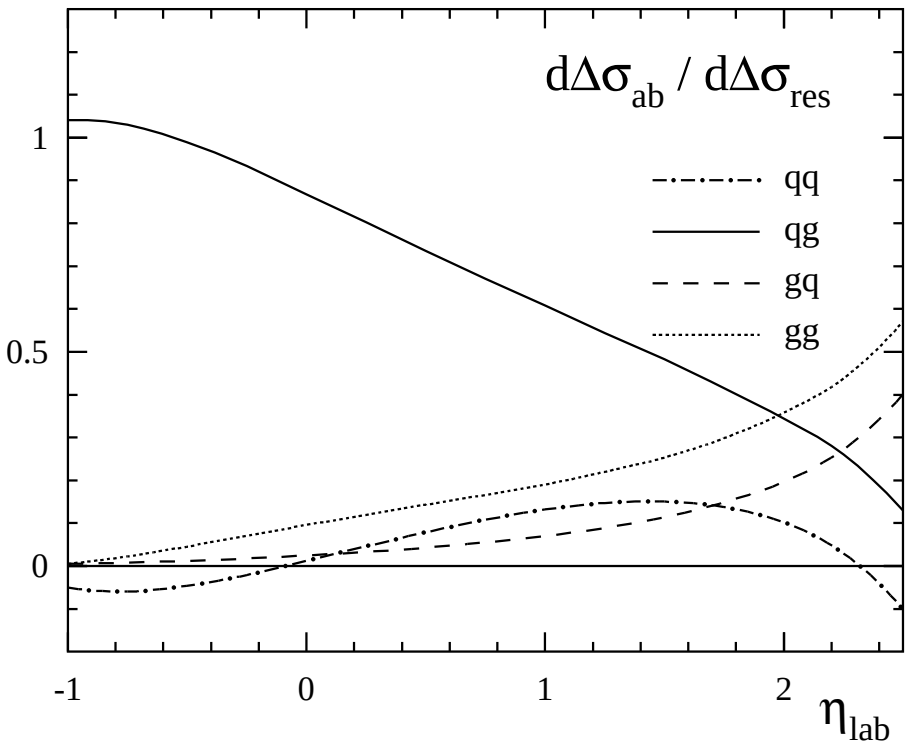

Figure 6: Relative contributions of different partonic scatterings $ab \to cX$ to the NLO ($\overline{\rm MS}$) resolved photon cross section for π^0 production at eRHIC, using the "standard" set of GRSV [16] for the proton and the "maximal" scenario for the spin-dependent photon densities.

structure of the nucleon to be known with much better accuracy than at present.

Figure 6 illustrates how different partonic scatterings $ab \to cX$ contribute to the NLO ($\overline{\rm MS}$) polarized resolved cross section, versus rapidity. Recall that parton "a" emerges from the photon and parton "b" from the proton. Qualitatively similar results are obtained for the "minimal" photon scenario and hence not shown here.

IV Conclusions

In this paper we have presented the first complete NLO calculation for the spin-dependent photoproduction of inclusive high-p_T hadrons, consistently including the direct and resolved photon contributions at NLO. Our results are relevant for future polarized lepton-proton collider projects like eRHIC, to which we have tailored our numerical results. The spin asymmetry for this process is a promising tool for a first determination of the spin structure of circularly polarized photons. We found that the QCD corrections to the polarized cross section are under good control. The polarized cross section shows a significant reduction of scale dependence

when going from LO to NLO.

We finally note that a single process alone, like pion photoproduction, will allow to establish the very existence of a polarized resolved-photon contribution and may perhaps point towards one of the two scenarios discussed above. It will, however, not be sufficient to fully disentangle the various quark flavor distributions and the gluon density of the polarized photon. This will require, as for the nucleon (spin) structure, a multitude of processes, combined in a global QCD analysis. Of course, at eRHIC other photoproduction processes, like jets, di-jets, or heavy flavors, will add further valuable information. Measurements at a future polarized linear e^+e^- collider would be also extremely helpful in this respect.

Acknowledgments

We are grateful to A. Deshpande for many valuable discussions about the eRHIC project. We thank A. Schäfer for discussions. B.J. and M.S. thank the RIKEN-BNL Research Center for hospitality and support during the final stages of this work, and they acknowledge support from the Program Development Fund PD02-98 of Brookhaven Science Associates. B.J. was supported by the European Commission IHP program under contract number HPRN-CT-2000-00130. W.V. is grateful to RIKEN, Brookhaven National Laboratory and the U.S. Department of Energy (contract number DE-AC02-98CH10886) for providing the facilities essential for the completion of this work. This work was supported in part by the "Bundesministerium für Bildung und Forschung (BMBF)" and the "Deutsche Forschungsgemeinschaft (DFG)".

References

[1] See, for example: G. Bunce, N. Saito, J. Soffer, and W. Vogelsang, Annu. Rev. Nucl. Part. Sci. **50**, 525 (2000).

[2] See discussions in: J.F. Owens, Phys. Rev. **D21**, 54 (1980);
M. Drees and R.M. Godbole, Phys. Rev. Lett. **61**, 682 (1988); Phys. Rev. **D39**, 169 (1989).

[3] A recent review can be found, e.g., in: M. Klasen, Rev. Mod. Phys. **74**, 1221 (2002).

[4] See `http://www.bnl.gov/eic` for information concerning the eRHIC/EIC project, including the "Whitepaper" BNL-68933.

[5] M. Stratmann and W. Vogelsang, Z. Phys. **C74**, 641 (1997);
J.M. Butterworth, N. Goodman, M. Stratmann, and W. Vogelsang, in proceedings of the workshop on "Physics with Polarized Protons at HERA", Hamburg, Germany, 1997, p. 120 [`hep-ph/9711250`].

[6] B. Jäger, A. Schäfer, M. Stratmann, and W. Vogelsang, Phys. Rev. **D67**, 054005 (2003).

[7] D. de Florian, Phys. Rev. **D67**, 054004 (2003).

[8] D. de Florian and W. Vogelsang, Phys. Rev. **D57**, 4376 (1998).

[9] D. de Florian and S. Frixione, Phys. Lett. **B457**, 236 (1999).

[10] F. Aversa, P. Chiappetta, M. Greco, and J.-Ph. Guillet, Nucl. Phys. **B327**, 105 (1989).

[11] P. Aurenche, R. Baier, A. Douiri, M. Fontannaz, and D. Schiff, Nucl. Phys. **B286**, 553 (1987).

[12] L.E. Gordon, Phys. Rev. **D50**, 6753 (1994).

[13] M. Glück, E. Reya, and A. Vogt, Phys. Rev. **D45**, 3986 (1992).

[14] M. Stratmann and W. Vogelsang, Phys. Lett. **B386**, 370 (1996).

[15] CTEQ Collaboration, H.-L. Lai *et al.*, Eur. Phys. J. **C12**, 375 (2000).

[16] M. Glück, E. Reya, M. Stratmann, and W. Vogelsang, Phys. Rev. **D63**, 094005 (2001).

[17] B.A. Kniehl, G. Kramer, and B. Pötter, Nucl. Phys. **B582**, 514 (2000).

[18] S. Kretzer, Phys. Rev. **D62**, 054001 (2000).

[19] PHENIX Collaboration, S.S. Adler *et al.*, hep-ex/0304038.

[20] M. Glück and W. Vogelsang, Z. Phys. **C55**, 353 (1992); *ibid.* **C57**, 309 (1993); M. Glück, M. Stratmann, and W. Vogelsang, Phys. Lett. **B337**, 373 (1994).

[21] M. Glück, E. Reya, and A. Vogt, Phys. Rev. **D46**, 1973 (1992).

[22] M. Glück, E. Reya, and C. Sieg, Phys. Lett. **B503**, 285 (2001).